Hydrodynamic performance of semi-pelagic self-adjusting otter boards in demersal trawl fisheries

Eighani, Morteza; Veiga-Malta, Tiago; O'Neill, Finbarr G.

Published in:
Ocean Engineering

Link to article, DOI:
10.1016/j.oceaneng.2023.113877

Publication date:
2023

Document Version
Publisher's PDF, also known as Version of record

Ocean Engineering 272 (2023) 113877

Contents lists available at ScienceDirect

Ocean Engineering

journal homepage: www.elsevier.com/locate/oceaneng

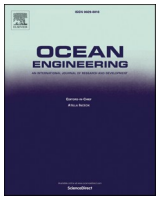

Hydrodynamic performance of semi-pelagic self-adjusting otter boards in demersal trawl fisheries

Morteza Eighani *, Tiago Veiga-Malta, Finbarr G. O'Neill

National Institute of Aquatic Resources (DTU AQUA), Technical University of Denmark, North Sea Science Park, 9850, Hirtshals, Denmark

ARTICLE INFO

Handling Editor: Prof. A.I. Incecik

Keywords:
Self-adjusting
Semi-pelagic trawl doors
Seabed contact
Low impact trawls
Fuel efficiency

ABSTRACT

In this study, we show how a novel self-adjusting, semi-pelagic otter board have high hydrodynamic efficiency and reduce seabed contact. The otter boards have two adjustable flaps, which are controlled by on-board altimeters and actuators, modifying their lift and drag and altering their position in the water column. The actuators are governed by a Proportional Integral Derivative feedback system, which uses the altimeter data to maintain the otter boards at a preset target height above the seabed.

Full-scale experimental trials were conducted to measure the hydrodynamic performance of this new design system and to compare it with a conventional seabed-contacting design. We demonstrate that the new system is highly efficient and has a lift/drag ratio of 4.2, which is 3.5 times that of the conventional otter boards. When the target height was set at 1 m, the SAO contacted the seabed at most 16% of the time; this decreased to 8% when the target height was raised to 2 m above the seabed; and there was no seabed contact when the target height was set at 5 and 10 m.

1. Introduction

Demersal trawling is responsible for about 20 million tonnes (approximately 25%) of global catch (Amoroso et al., 2018; Pérez Roda et al., 2019) and makes a significant contribution to food security. Furthermore, it is a key economic driver, a major source of employment, and vital to the cultural identity of many coastal communities worldwide (FAO, 2018).

Otter boards (or trawl doors) are a key component of demersal trawl fishing gears. The hydrodynamic lift forces they generate spread the net and keep it open, consequently, they affect the fishing efficiency and economic effectiveness of the fishing operation. Their drag forces, however, can account for up to 30% of the total-system drag (Sterling and Eayrs, 2010) and the associated turbulence can mobilize sediment into the water column (O'Neill and Summerbell, 2011; 2016). They are also one of the heaviest components of a trawl gear and contribute to getting the gear down to the seabed quickly after deployment and to ensuring that the gear maintains contact with the seabed while fishing. However, they can penetrate the seabed, displace and compact sediment and modify the benthic habitat. Hence, a well-designed otter board will maximize its hydrodynamic efficiency (lift/drag ratio) while minimizing its physical impact on the seabed.

Traditional demersal otter boards have a low aspect ratio (height/length < 1.0) and maximum hydrodynamic efficiencies in the range 1.2–1.7 (SEAFISH et al., 1993). Many studies have been conducted to improve their design, stability and hydrodynamic efficiency (Reite and Sørensen, 2004; Prat et al., 2008; Sala et al., 2009). There have also been many developments of high aspect ratio otter boards, which can have significantly higher lift-to-drag ratio. Studies of bi-plane and multi-wing otter boards show that they have a better overall hydrodynamic efficiency than traditional monoplane and one-panel structures (Takahashi et al., 2015; Wang et al., 2021, 2022; Su et al., 2018; Zhuang et al., 2022), and some of the most efficient designs have lift-to-drag ratios of up to 4.4 (You et al., 2021; Liu et al., 2017; Xu et al., 2021; Chu et al., 2020).

In order to reduce seabed contact, semi-pelagic otter boards that have been towed above the seabed and, in principle, do not contact it have also been developed (DeLouche and Legge, 2004; Reite and Sørensen, 2006; He et al., 2006; Eayrs, 2014; Grimaldo et al., 2015; Sistiaga et al., 2015). However, using semi-pelagic otter boards without proper control on the position of them in the water column can result in seabed contact particularly on a varying seabed or during poor weather conditions (Eayrs and CraigShort, 2020).

In this study, we measure the hydrodynamic performance of a novel

* Corresponding author.
E-mail address: moei@aqua.dtu.dk (M. Eighani).

https://doi.org/10.1016/j.oceaneng.2023.113877
Received 29 November 2022; Received in revised form 17 January 2023; Accepted 3 February 2023
Available online 7 February 2023

Fig. 1. The semi-pelagic self-adjusting, otter boards (SAO) during sea trials.

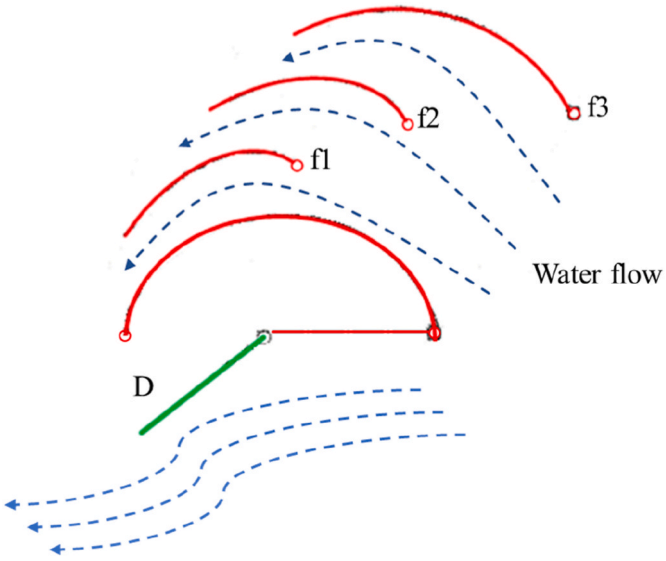

Fig. 2. Cross sectional view of the main structural elements of the SAO where f1, f2, and f3 are the curved static foils and D is one of the adjustable flaps.

self-adjusting, semi-pelagic otter board (SAO) system that has been developed by MLD Trawls, Esbjerg, Denmark (Fig. 1). These doors incorporate some of the recent design features mentioned above to maximize hydrodynamic performance. Furthermore, they minimize contact with the seabed in demersal trawl fisheries as, uniquely, they have onboard altimeters and adjustable flaps that are controlled by an active Proportional-Integral-Derivative (PID) feedback system. The PID system modifies the position of the doors in the water column by adjusting the flap openings via actuators by comparing the altimeter data to a pre-set target height above the seabed. We measure, under operational conditions at sea, the hydrodynamic efficiency, the spreading and drag forces and the extent to which the doors avoid contact with the seabed.

2. Methods

2.1. Self-adjusting, otter boards (SAO)

The design of the SAO is centered around three curved static foils which enhance the hydrodynamic performance of the otter boards by delaying the appearance of flow separation (Xu et al., 2018; Wang et al., 2021). There are also two flaps on each otter board that can be rotated from zero to 45° by actuators (Figs. 2 and 3). When the lower flap is open, the otter boards rolls forward and moves in the upward direction (Fig. 3a); when the upper flap is open, the otter boards rolls backwards and moves in the in downward direction (Fig. 3b); and when both flaps are open, the spreading forces increase and the otter boards move in the horizontal direction (Fig. 3c). The heights of the otter boards above the seabed are measured acoustically by altimeters, and these measurements are used by a Proportional-Integral-Derivative (PID) feedback system to control the extent to which the upper and lower flaps are open in order to maintain pre-set height targets.

The dimensions of the otter boards are presented in Table 2, where the length of the SAO is defined to be the distance from the forwardmost point of the leading edge of the otter board to the furthermost point of the side with the flap (Fig. 3c). The angle of attack of the SAO is defined to be the angle between this later side and the direction of tow. It is determined by the rigging points used (Fig. 4a), which were those proposed by the manufacturer, giving an angle of attack for the SAO of 16°.

2.2. Experimental trials

The trials were carried out in the Kattegat and Skagerrak Seas onboard RV "Havfisken" (17 m L.O.A., 373 kW engine power) in the autumn of 2021. All trials took place in the same area where water depth varied from 35 to 42 m and the substrata was muddy sand.

The fishing gear towed was a two-panel demersal trawl with a mesh size of 134 mm constructed of 2.5 mm PE twine and had a twine area of 42.44 m^2 (Fig. 5). The headline of the trawl was 27 m and was fitted with 41 spherical 20 cm diameter floats. The 20 m ground gear was composed of two 6 m sections of 14 rubber discs (14.5 cm in diameter and 29 mm thick) and an 8 m central section of 73 rubber discs (14.5 cm in diameter and 10 mm thick) (Fig. 6). The codend had a 120 mm mesh size (nominal) made of 3 mm PE double twine. It was 50 meshes long and 80 meshes in circumference and was kept open during the trials to avoid any influence of catch weight. The sweep and bridle rigging is shown in Fig. 7.

This gear was towed with the SAO set at four different target-height settings (1, 2, 5 or 10 m), each of which was examined with sweep lengths of 55 m and 110 m (half and full sweeps, respectively). Cambered V-type seabed-contacting otter doors (Thyborøn type 2), which are commonly used in Danish demersal fisheries, were selected as reference doors, and were also tested with sweep lengths of 55 m and 110 m, giving, in total, 10 configurations (Table 3). Conventional door was rigged at their proposed industry-standard angle of attack (Fig. 4b). Each configuration was tested over two legs, (with and against the tide), where each leg comprised of tows at three nominal speeds (2.5, 3.0, and 3.5 knots). Three minutes were allowed to let the gear settle between speed changes, after which, 10–15 min of the following measurements were recorded.

The tensions in the warps and sweeps immediately before and after the doors were measured by four 5 tonne Strainstall wireless load shackles. The speed of the gear through the water was measured by a Valeport current meter (model 106) attached to the center of the trawl headline. Simrad acoustic instrumentation measured net and gear geometry including headline and wing-end heights, otter board, and wing-end spreads. A Garmin GPS unit output vessel position, ground speed,

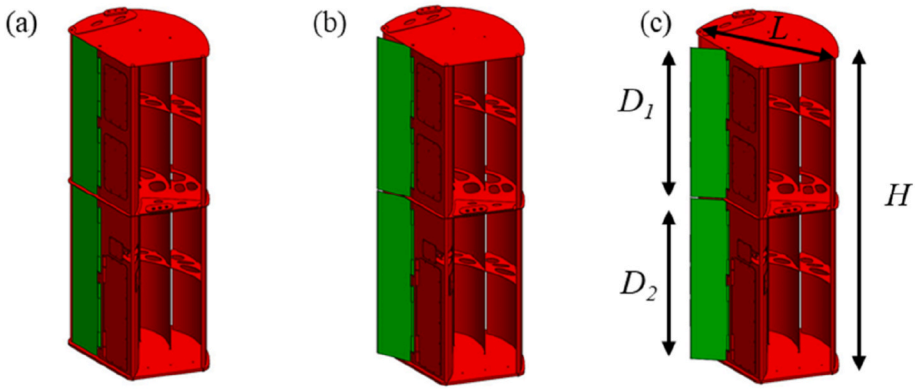

Fig. 3. Schematic view of the SAO; (a) when the angle of the lower flap is greater than that of the upper one, the otter board rolls forward and goes higher in the water column (b) when the angle of the upper flap is greater than that of the lower one, the otter board rolls backwards and goes lower in the water column, (c) when both flaps are open the horizontal spreading forces increase. Length and height, L and H, are respectively 0.79 and 2.20 m. Length of upper and lower flaps, D_1 and D_2, are 1.03 and 1.11 m.

Table 1
Hydrodynamic performance comparison among different types of otter boards.

otter board type	Study	Maximum lift/ drag ratio
vertical cambered	Flume Tank (Zhang et al., 2004)	4.6
Clarck-Y	Full scale (Sala et al., 2009)	3.6
biplane-type	Flume Tank (Takahashi et al., 2015)	3.3
double-slotted cambered	Wind tunnel (Wang et al., 2017)	3.8
oval cambered double slotted	Flume Tank (Liu et al., 2017)	4.1
Double deflector rectangular cambered	Flume Tank (Xu et al., 2018)	3.7
double-winged	Flume Tank (Su et al., 2018)	1.8
Grilli Fly	Flume Tank (Mellibovsky et al., 2018)	3.7
Thyborøn type 15 vf	Flume Tank (Mellibovsky et al., 2018)	3.6
otter board with a trailing edge flap	Flume Tank (Lee et al., 2019)	2.6
double-slotted vertical cambered V-type	Numerical simulation (Chu et al., 2020)	4.1
Batwing	Full scale (Balash et al., 2020)	3
rectangular cambered	Numerical simulation (Xu et al., 2021)	4.1
Wingtip-blocked cambered	Flume Tank (You et al., 2021)	4.4
multi-wing	Wind tunnel (Wang et al., 2021)	3.6
biplane hyper-lift	Flume Tank (Zhuang et al., 2022)	2.8
Double-Vane	Wind tunnel (Wang et al., 2022)	3.1
Thyborøn type 2	Flume Tank (SEAFISH et al., 1993)	1.5

Table 2
Characteristics of the SAO and Thyborøn type 2 otter boards used in the experimental trials.

Parameter	SAO	Thyborøn type 2
Length (m)	0.79	1.70
Height (m)	2.20	1.05
Area (m^2)	1.74	1.78
Aspect ratio	2.78	0.62
Weight in air (kg)	300	360

and water depth and a Furuno Doppler Sonar current indicator (model CI-88) measured tide speed and direction. The warp and sweep yaw angles, γ and σ respectively, (from the warp and sweep to the horizontal plane) were measured with Star-Oddi DST tilt sensors.

For each tow, the rate of fuel consumption was recorded every 3 s using the vessels fuel meter. Video footage of each otter door was collected using two Paralenz dive cameras attached to the upper backstrop, approximately 1 m behind the otter boards, and illuminated with LED lights. The footage was subdivided into 3-s intervals, and an interval was defined as 'contacting the seabed' if during those 3 s there was a door-seabed interaction that caused a sand cloud.

2.3. Calculation of drag and lift coefficients

The components of the warp and sweep tensions were resolved into their vertical and horizontal components to calculate the spreading and drag forces. The warp and sweep pitch angles, θ and ε respectively, were calculated as follows

$$\theta = \sin^{-1}\left(\frac{d_s - b_w}{2w_l}\right)$$

$$\varepsilon = \sin^{-1}\left(\frac{d_s - w_s}{2s_l}\right)$$

where d_s is the door spread, b_w is the block width, w_l is the warp length, w_s is the wing-end spread and s_l is the sweep length.

Hence the horizontal components of the warp and sweep tensions in the direction of tow are

$$W_x = W \cos\gamma \cos\theta$$

$$S_x = S \cos\varepsilon \cos\sigma$$

and the *corresponding* horizontal spreading (lift) components are

$$W_y = W \cos\gamma \sin\theta$$

$$S_y = S \cos\varepsilon \sin\sigma$$

We define 'gear drag', D_G, to be the sum of the port and starboard horizontal components of the warp tensions in the direction of tow and define 'net drag', D_N, to be the sum of the corresponding components of the sweep tensions. Hence, gear drag comprises the drag of the doors, sweeps, groundgear and netting, while the net drag comprises the drag of the sweeps, groundgear and netting, hence,

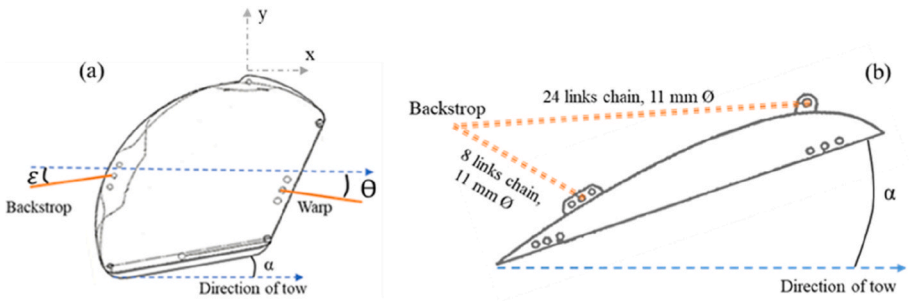

Fig. 4. Definition of the angles on orientation of the otter board in the water. (a) top view of the SAO and (b) top view of the conventional door. Angle of attack (α), warp pitch angle (θ), sweep pitch angle (ε).

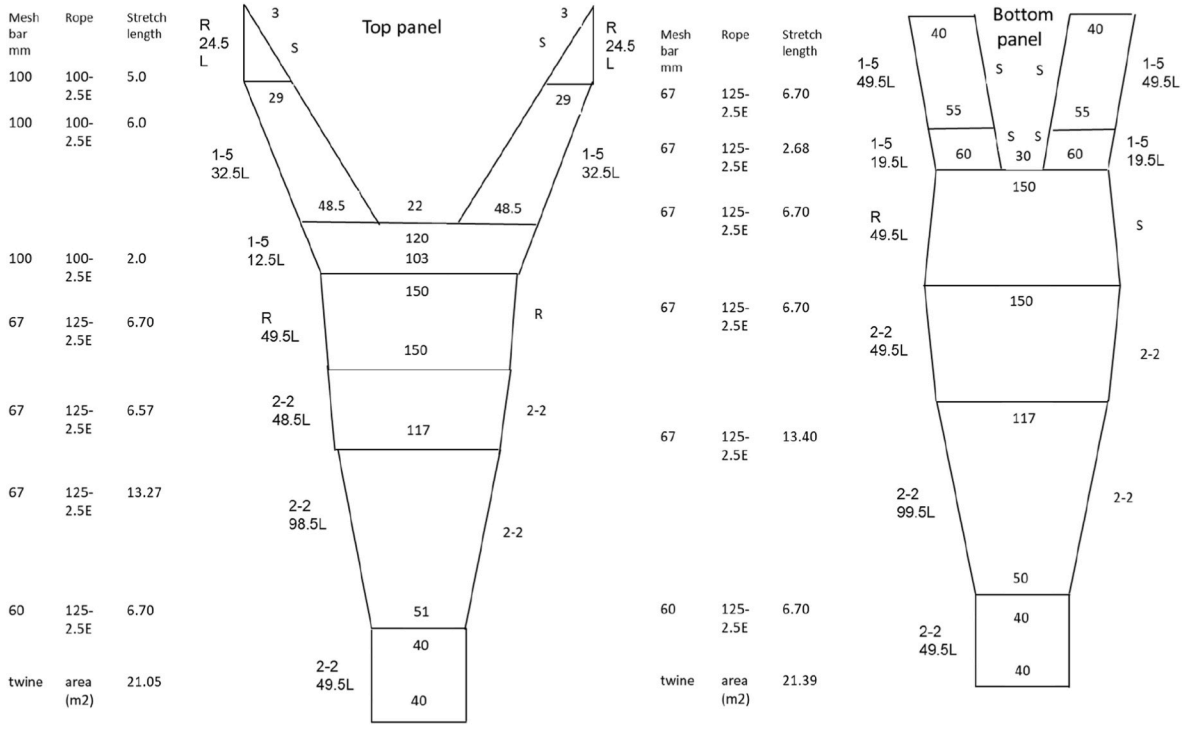

Fig. 5. Plans of the two-panel demersal trawls used in the study.

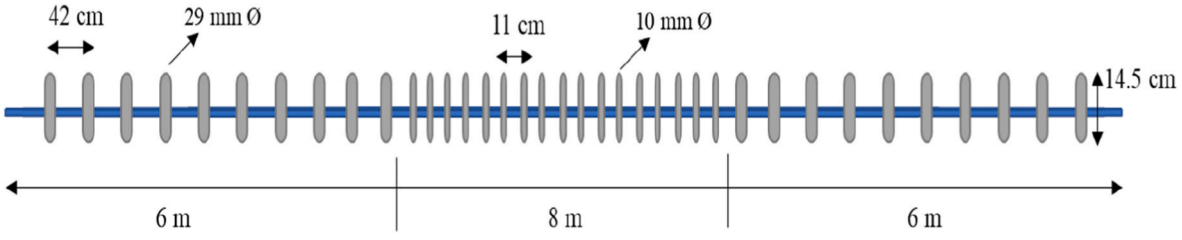

Fig. 6. Design of groundgear used in the sea trial.

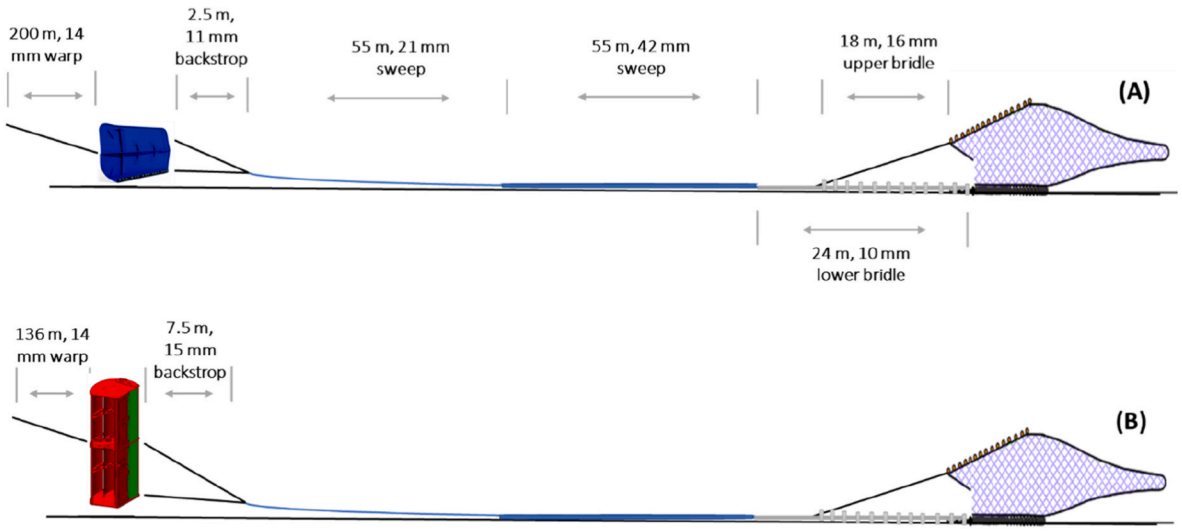

Fig. 7. Schematic view of the sweep and bridle rigging arrangement used during the sea trials. Conventional otter board (A) and the SAO (B). By shifting from conventional to the SAO, only backstrop and warp were changed.

Table 3
Summary of sets for comparing the SAO and conventional otter boards in full-scale trials in North Sea demersal trawl fisheries.

Otter board Type	Sweep Rig	No of tows	Warp length (m)	Water depth (m)	Target door height (m)	Target speed (kts)	Wind speed (m/s)
Con	Full (110 m)	6	200	38.2 ± 1.9	0	2.5, 3.0, 3.5	4.2 ± 0.6
Con	Half (55 m)	6	200	37.9 ± 1.8	0	2.5, 3.0, 3.5	2.8 ± 0.4
SAO	Full (110 m)	23	136	39.2 ± 2.8	1, 2, 5, 10	2.5, 3.0, 3.5	8.9 ± 1.2
SAO	Half (55 m)	16	95	37.4 ± 0.5	1, 2, 5, 10	2.8, 3.3	7.0 ± 0.9

Table 4
The best fit models as selected using the lowest AIC. The explanatory variables in bold have a significant effect ($p < 0.05$).

Response variables	Expression
Gear drag	**doortype** + **speed** + **current** + **sweep** + sweep:doortype + **speed:doortype** + (1 | Tow)
Net drag	doortype + **speed** + **current** + sweep + sweep:doortype + **speed:doortype** + (1 | Tow)
Door drag	**doortype** + **speed** + current + **sweep** + sweep:doortype + **speed:doortype** + (1 | Tow)
Drag coefficient	**doortype** + **speed** + **speed:doortype** + (1 | Tow)
Lift coefficient	**doortype** + **speed** + **speed:doortype** + (1 | Tow)
Efficiency	**doortype** + speed + speed:doortype + (1 | Tow)
Door spread	**doortype** + **speed** + **sweep** + **sweep:doortype** + **speed:doortype** + (1 | Tow)
Wing spread	**doortype** + **speed** + **sweep** + **sweep:doortype** + **speed:doortype** + (1 | Tow)
Headline height	**doortype** + speed + **doorheight** + **sweep** + **sweep:doortype** + **speed:doortype** + (1 | Tow)
Fuel consumption	**doortype** + **speed** + **current** + sweep + sweep:doortype + **speed:doortype** + (1 | Tow)

Note. Doortype is a categorical variable (SAO or conventional); speed is a continues variable; doorheight is a categorical variable (target heights of 1, 2, 5 and 10 m); current is a categorical variable (with and against current); and sweep is a categorical variable (full (110 m) and half (55 m) sweep lengths).

$$D_G = W_{xp} + W_{xs}$$

$$D_N = S_{xp} + S_{xs}$$

where the p or s, in a subscript refers to port or starboard. Accordingly, the average drag of the two doors is

$$D_D = (D_G - D_N)/2$$

Similarly, the average horizonal spreading force on a door is

$$L_D = \left(W_{yp} + W_{ys} + S_{yp} + S_{ys}\right)/2$$

The drag and lift coefficients (C_D and C_L) and the efficiency (η), are defined as

$$C_D = 2gD_D/\rho V^2 A, C_L = 2gL_D/\rho V^2 A, \eta = C_L/C_D$$

where ρ is the fluid density (1026 kg/m^3), g is the acceleration due to gravity (9.8 m/s^2), V is the speed through the water (m/s) and A is the area of otter board (m^2).

2.4. Statistical analyses

The response variables of the net, gear and door drags, the drag and lift coefficients, the hydrodynamic efficiency, the door spread, wing spread and headline height, and the fuel consumption data were first explored using the methods described in Zuur et al. (2010). This included detecting outliers in the data, testing for homogeneity of variance and normality, as well as testing for the existence of correlation among the following explanatory variables: door type, target door height, speed through the water, current direction, and sweep length (Table 4). Data smoothing by the moving average method with five windows is applied for the speed and tension measurements in order to remove noise in the data.

Generalized linear mixed effects models (GLMM) with a Gaussian distribution were used to model each of the response variables in terms of the explanatory variables (Zuur et al., 2013). Multiple tows were completed by specific door type, and data from each door type were nested between the tows. Thus, we treated tows as a random effect (i.e. observations from different sets from the same door type). The mixed effect model's structure was:

$$Y = X_{\beta} + Z_H + \mathrm{q}$$

Where Y is the response variable; X is the vector of the explanatory

Table 5
Estimated values of hydrodynamic drag, and fuel consumption (FC) respect to different sweep configurations, tide current, and speeds. Conventional (Con) and self-adjusting otter board (SAO).

Sweep rig	Tide current	Door type	Speed (m/s)	Tide speed (m/s)	RPM	Gear drag (kgf)	Net drag (kgf)	Door drag (kgf)	FC (L/H)
Full	Opposite	Con	1.28	0.07	1200	1504	1131	186.5	18.9
			1.54	0.09	1300	2013	1439	277	30.4
			1.81	0.08	1400	2535	1769	382.5	40.1
		SAO	1.28	0.53	1300	1385	1211	92.5	20.4
			1.54	0.56	1400	1711	1519	110	29.3
			1.81	0.50	1500	2101	1855	142.5	37.8
	With	Con	1.28	0.11	1200	1409	1066	180	22.9
			1.54	0.10	1300	2044	1458	278.5	31.9
			1.81	0.08	1400	2431	1730	372	40.7
		SAO	1.28	0.23	1200	1147	1011	75.5	14.4
			1.54	0.21	1300	1663	1472	112.5	21.3
			1.81	0.21	1400	2011	1783	134.5	27.1
Half	Opposite	Con	1.28	0.09	1200	1541	1119	207	22.2
			1.54	0.10	1300	2052	1397	300	32.6
			1.81	0.07	1400	2620	1799	413	41.8
		SAO	1.28	0.10	1350	1255	1099	89.5	16.9
			1.54	0.10	1400	1603	1376	118.5	23.9
			1.81	0.10	1450	1943	1700	144	29.6
	With	Con	1.28	0.20	1200	1470	1060	199	22.9
			1.54	0.12	1300	1897	1354	279.5	32.3
			1.81	0.17	1400	2449	1618	405.5	41.5
		SAO	1.28	0.20	1350	1239	1088	85.5	15.8
			1.54	0.15	1400	1571	1373	110.5	22.1
			1.81	0.15	1450	1933	1666	139.5	27.9

variables; ß are the fixed-effects regression coefficients; and Ɋ are the residuals, while Z and H are the matrix of covariates and the corresponding vector of random effects. H is assumed to follow a normal distribution, and therefore, Var(Y) = Var(H) + Var(Ɋ). The variance components are estimated by the method of restricted maximum-likelihood (REML) (Patterson and Thompson, 1971), which sets unbiased estimates for the variance components. The mixed effect model was implemented using the 'lme4' package in R (Bates et al., 2014; R Core Team, 2020). All possible combinations of the model were fitted using the function "dredge" from the package 'MuMIn' (version 1.43.17, Barton, 2022) and the model with the lowest Akaike information criterion (AIC) value was selected (Akaike, 1974).

Model validation was applied to investigate the presence of any residual patterns. This was confirmed by visual inspection of the plots for the posterior mean Pearson residuals versus posterior mean fitted values, versus each explanatory variable for patterns (Zuur and Ieno, 2016). In addition, to verify normality, we made histograms of the residuals.

3. Results

In total, 51 tows were carried out, with different combinations of door type, target door height, speed through the water, current direction, and sweep length (Table 3). The spreading force of the SAO was such that to counter overspreading it was necessary to reduce the warp length (from 200 to 136 m) during tows when they were used.

3.1. Hydrodynamic performance

The SAO target height above the seabed did not appear in any of the models related to the hydrodynamic performance of the doors.

The gear drag depends on door type, the current direction, the sweep length and speed. It is significantly lower for the SAO than for the conventional door, with about an 18% difference at 3.0 knots (Table 5, Fig. 8). The net drag depends only on the speed and current direction and there is no significant dependency on either the door type or the sweep length ($p > 0.05$). The door drag is significantly affected by the door type, speed, and sweep length, and the drag of the SAO is about 59% lower than that of the conventional door at 3.0 knots ($p < 0.05$) (Fig. 7). As would be expected, all three drags increase with increasing speed (Table 5; Fig. 8).

The drag coefficient (C_D) of the SAO is significantly lower than that of the conventional door, with a difference of about 60% at 3.0 knots (Table 6; $p < 0.05$). Further, while the C_D of the SAO decreases with speed, that of the conventional door remains constant (Fig. 9). Contrastingly the lift coefficient (C_L) of the SAO is significantly greater than that of the conventional door, and is about 34% larger at 3 knots. C_L of both doors decreases with an increase in the speed but the decline is steeper for the SAO (Table 6; $p < 0.05$). The efficiency (lift/drag ratio) of both doors is approximately constant. The SAO value is on average 4.2, whereas that of the conventional door is 1.2. Hence, the efficiency of the SAO is 3.5 times that of the conventional door (Fig. 9).

3.2. Gear geometry

The door and wingend spreads are dependent on the door type, speed, and sweep length. They are respectively 10 and 7% greater for the SAO in comparison to the conventional door at 3.0 knots (Table 7; $p < 0.05$) (though this effect is not significant in half sweep rig). There is no significant difference in headline height of the trawl net between the SAO at target heights of 1, 2, and 5 m, and the conventional door, in the full sweep rig. However, there is a significant difference for the SAO at the 10 m target height ($p < 0.05$). For the half sweep rig, the SAO with target heights of 5 and 10 m also has a significantly higher headline

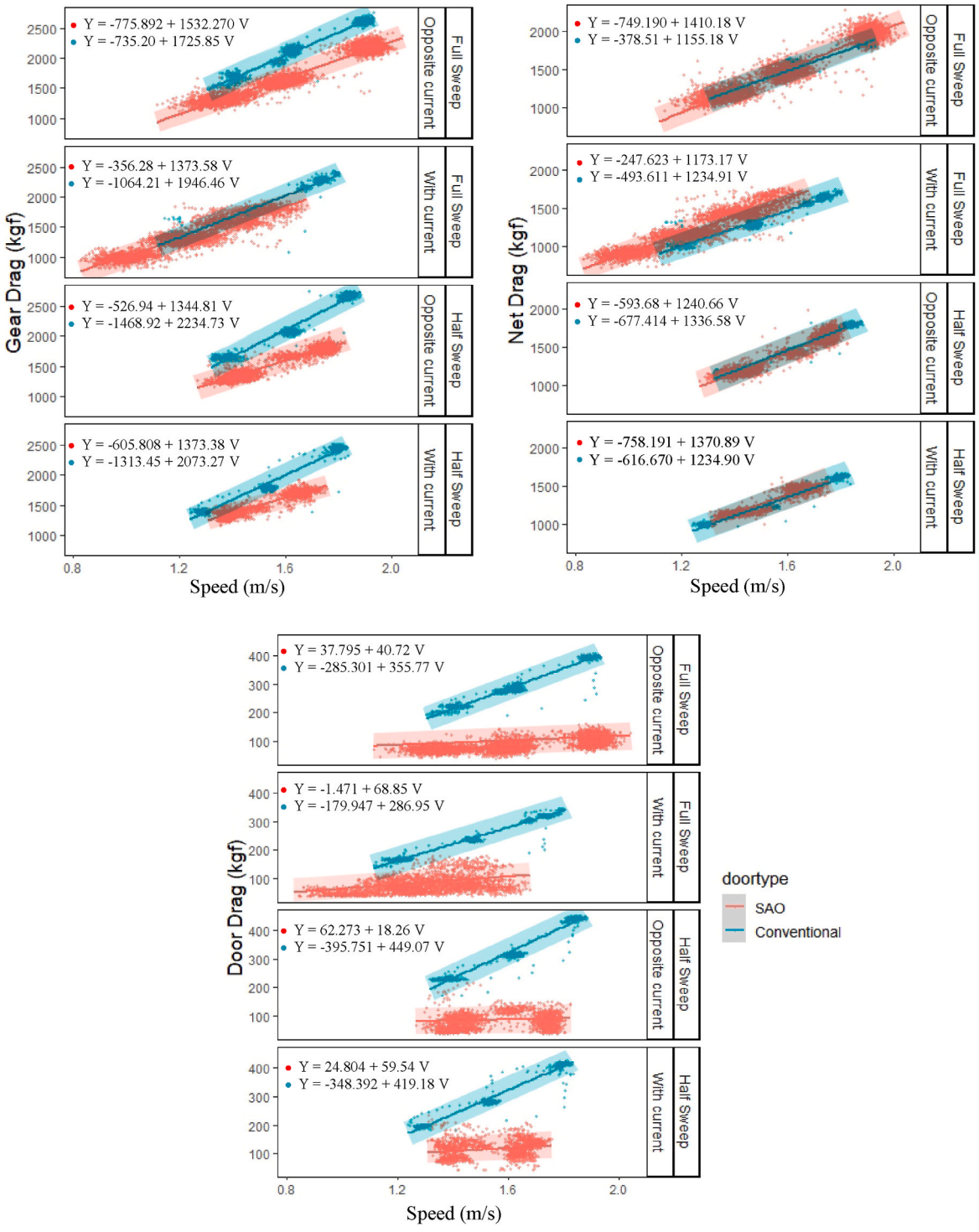

Fig. 8. Estimated curve for comparing gear, net, and door drags (kgf) between door types. Points represented experimental observations and shaded area represented 95% confidence interval.

Table 6
Estimated values of hydrodynamic coefficients respect to different towing speeds. Conventional (Con) and self-adjusting otter board (SAO), drag coefficient (C_D), lift coefficient (C_L), efficiency of otter board (Eff), sweep pitch angle (ϵ), warp pitch angle (Θ), tilt angle of the otter board (φ).

Door type	Speed (m/s)	C_D	C_L	Eff	ϵ	Θ	φ
Con	1.28	1.25	1.63	1.32	14.8	7.7	9.7
	1.54	1.25	1.51	1.21	15.6	8.4	10.3
	1.81	1.26	1.36	1.09	16.2	8.7	15.5
SAO	1.28	0.61	2.59	4.26	15.3	14.2	8.1
	1.54	0.48	2.02	4.25	16.1	15.7	9.2
	1.81	0.41	1.73	4.31	17.3	16.3	11.6

height than conventional door (Table 7; $p < 0.05$).

3.3. Fuel consumption

There is a significant decrease of about 18% fuel consumption when the SAOs are used at 3.0 knots with full sweeps in comparison to the conventional door (Table 5; $p < 0.05$). In addition, results show that the fuel consumption increases with towing speed and when towing against the current (Fig. 10).

3.4. Seabed contact and flap angles

The position of the SAO above the seabed in relation to the target height is shown in Fig. 11a. When the target height was set at 1 m, the SAO contacted the seabed at most 16% of the time. Seabed contact decreased to 8% when the target height was raised to 2 m above the seabed, and there was no seabed contact when the target height was set at 5 and 10 m.

Fig. 11b shows that as the speed increases, there is a decrease in the frequency of open flaps (high angles) and an increase in the frequency of closed flaps (low angles).

4. Discussion

We have shown that the SAO, under operational conditions at sea, are highly efficient. They have high spreading forces and low drag, they reduce fuel consumption, and the PID system ensures that seabed contact can be minimized.

The SAOs have an average efficiency of 4.2, which places them as one of the most highly hydrodynamically efficient doors (see Table 1 for details). It also important when examining hydrodynamic performance to consider the lift characteristics. The SAO has a lift coefficient of 2.02 at 3.0 knots which compares well with other high-lift otter boards, which have maximum values in the range of 1.71–2.38 (Shen et al., 2015; Su et al., 2018; Xu et al., 2018; Wang et al., 2022). Furthermore, in comparison with conventional seabed-contacting doors, the SAO are 3.5 times more efficient and have a 34% greater C_L. These results are particularly noteworthy, given that there will be inefficiencies associated with the self-adjusting opening and closing of the flaps. This is especially the case when the flaps are more open at lower speed and there will be increased drag and lift forces (Fig. 11b). This explains why the C_D and C_L coefficients of the SAOs are higher at lower speeds (Fig. 8). Normally, it would have been expected that the drag coefficient would be constant over the speed (Reynolds number) range experienced here, but as shown in Fig. 10, the flaps of the SAO are more frequently open at lower speeds than at higher ones, resulting in a higher drag coefficient. In contrast, the drag coefficient of the conventional door is constant, which is consistent with a fixed geometry and fixed points of flow separation. The movement of the flaps also explains the greater amount of variability in the SAO measurements.

We have demonstrated there was no contact when the target height was set at 5 and 10 m above the seabed. Our estimates of contact regarding 1 and 2 m target heights are likely to be over-estimates as our method for defining contact are very conservative. This proves that the PID feedback system successfully controls position of the doors above the seabed. However, we should also be aware that these results will depend on seabed variability and sea state and require study over a broader range of operational conditions.

The drag of the SAO was 59% less than that of the conventional doors. This is due to both a reduction of their hydrodynamic drag and the fact that they have reduced contact drag. It results in a combined (doors, sweeps, groundgear and net) gear drag reduction of about 18% and a similar reduction in fuel consumption. We must, however, treat the fuel consumption results with caution, as they also account for the drag of the vessel and warps and will be influenced by tide, wind and sea state, and propeller pitch and rpms and hence must be assessed over a broader range of operational conditions. Nevertheless, they compare well with the results of other authors who found reductions in fuel consumption of between 12 and 22% when using doors of reduced contact or semi-pelagic doors (McHugh et al., 2015; Eayrs et al., 2012; Grimaldo et al., 2015).

The spreading force of the SAO was 34% greater than the conventional doors, and to counter overspreading it was necessary to reduce the warp length (from 200 to 136 m) when using the SAO. Further reduction of the warp length restricted the ability of the SAO to get close to the seabed. As a result, the door and wingend spreads are slightly greater when the SAO are used in comparison to the conventional doors. These results demonstrate that the SAOs could have been smaller, and a similar spreading force to the conventional doors would have been obtained if their linear dimensions were reduced by 14%, which in turn would lead to further drag reductions and fuel savings.

There was no difference in the headline height of the trawl net between the conventional door and the SAO when the target height of the SAO was set at 1, 2, and 5 m, but there was when the SAO had a target height of 10 m. This is relevant as it indicates that, when the doors are at this height, the fishing line may have risen from the seabed. This can affect the catching performance of the fishing gear and suggests that a 10 m target height should be avoided with the rigging arrangement tested here.

In summary, we have demonstrated that the self-adjusting otter board system reduces seabed contact and fuel consumption and improves the ecological performance of towed fishing gears and hence, will contribute to the economic and environmental sustainability of demersal fisheries.

CRediT authorship contribution statement

Morteza Eighani: Data curation, Methodology, Experimental, Validation, Formal analysis, Writing – original draft, manuscript. **Tiago Veiga-Malta:** Methodology, Experimental, Validation, Formal analysis, Writing – review & editing. **Finbarr G. O'Neill:** Conceptualization, Funding acquisition, Methodology, Experimental, Validation, Writing – review & editing, Supervision.

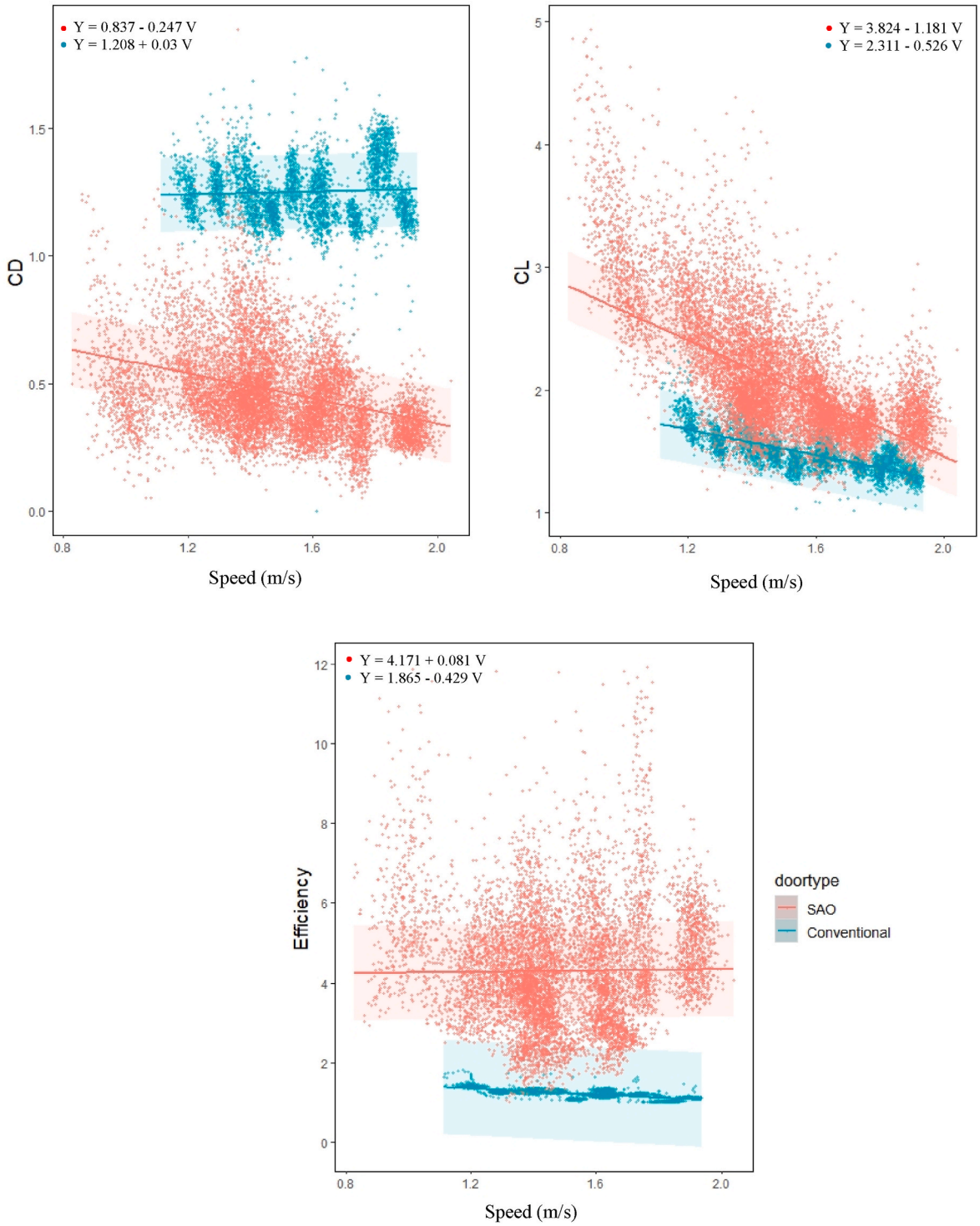

Fig. 9. Estimated curve for comparing drag and lift coefficients (C_D and C_L) and the hydrodynamic efficiency between door types. Points represented experimental observations and shaded area represented 95% confidence interval.

Table 7
Estimated values of gear geometry respect to different towing speeds and sweep rigs. Conventional (Con), self-adjusting otterboard (SAO), door spread (DS), wing spread (WS), headline height of the net with conventional door (HH_0), the SAO at 1 m target height (HH_1), the SAO at 2 m target height (HH_2), the SAO at 5 m target height (HH_5), and the SAO at 10 m target height (HH_{10}).

Sweep rig	Door type	Speed (m/s)	DS (m)	WS (m)	HH_0 (m)	HH_1 (m)	HH_2 (m)	HH_5 (m)	HH_{10} (m)
Full	Con	1.28	71.4	13.4	2.45	–	–	–	–
		1.54	73.9	13.5	2.23	–	–	–	–
		1.81	76.6	13.5	2.05	–	–	–	–
	SAO	1.28	79.8	14.5	–	2.58	2.60	2.68	2.42
		1.54	81.5	14.6	–	2.41	2.21	2.43	2.75
		1.81	83.4	14.7	–	2.13	1.83	2.17	3.10
Half	Con	1.28	54.5	13.8	2.53	–	–	–	–
		1.54	58.1	14.2	2.19	–	–	–	–
		1.81	61.6	14.5	1.86	–	–	–	–
	SAO	1.28	54.9	14.2	–	2.66	2.66	2.79	3.29
		1.54	53.5	13.9	–	2.57	2.62	2.88	4.70
		1.81	52.2	13.6	–	2.55	2.60	2.95	6.15

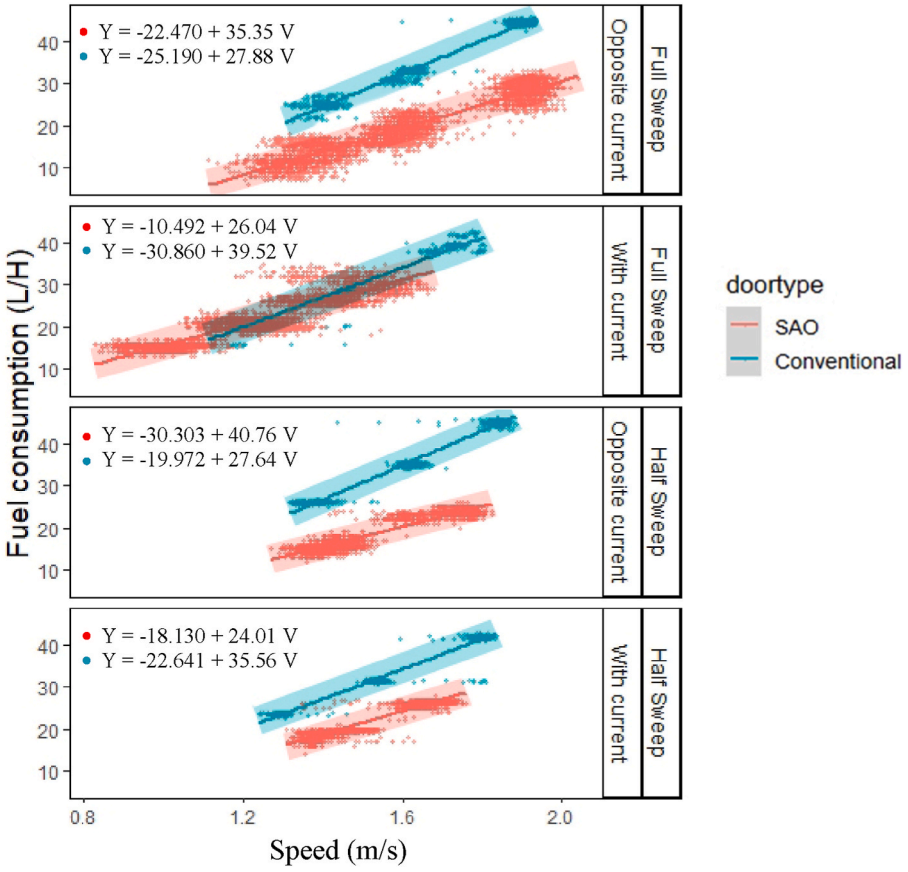

Fig. 10. Estimated curve for comparing fuel consumption between door types. Points represented experimental observations and shaded area represented 95% confidence interval.

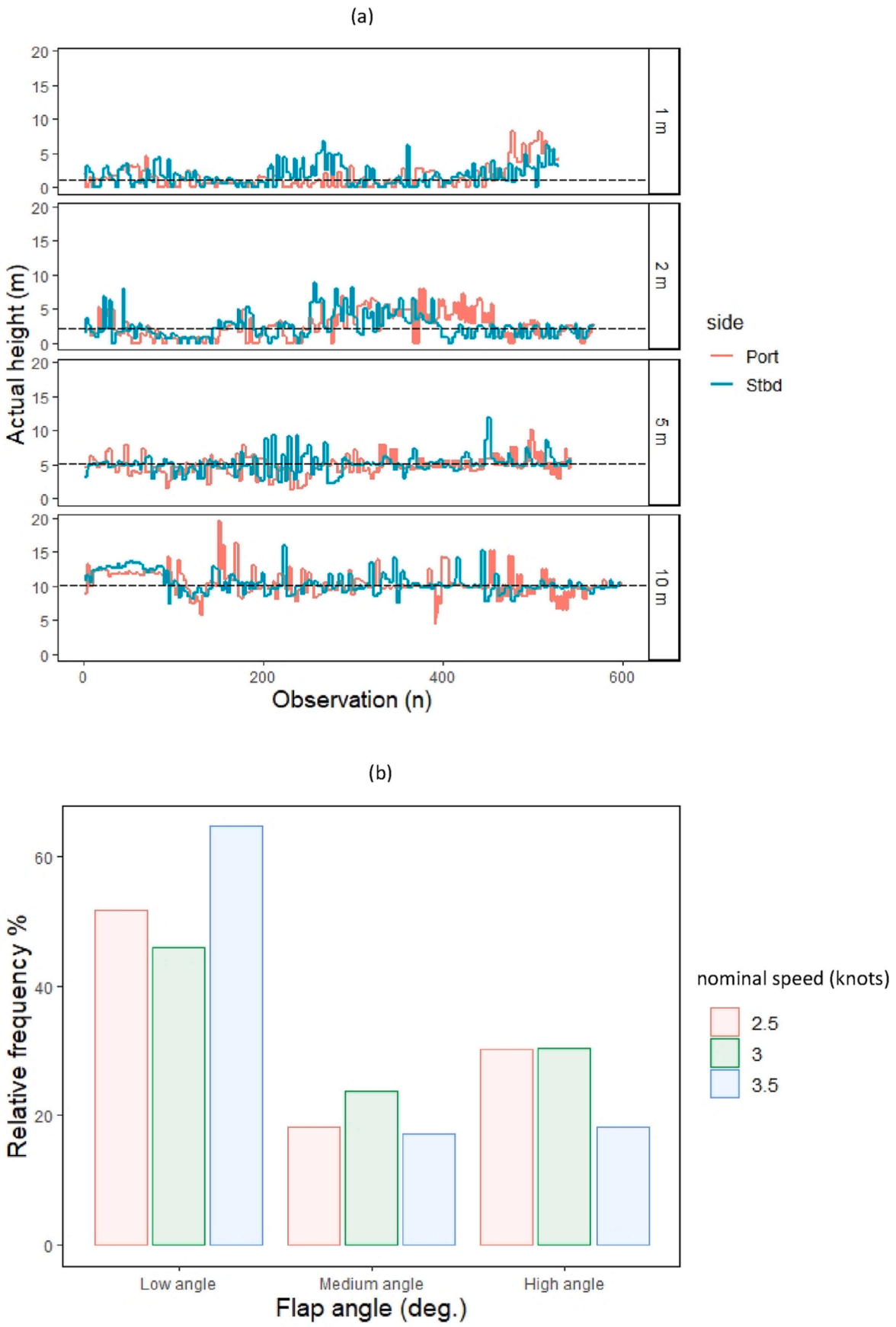

Fig. 11. (a) Actual height of the SAO in relation to the target door height. The black dashed line is the target height above the seabed. (b) The relative frequency the flap angles are in the ranges low (0–15°), medium (15–30°) and high (30–45°) at the different nominal speeds.

Declaration of competing interest

The authors declare the following financial interests/personal relationships which may be considered as potential competing interests: Barry O'Neill reports financial support was provided by Ministry of Environment and Food of Denmark through the Green Development and Demonstration Program (GUDP).

Data availability

Data will be made available on request.

Acknowledgments

This study received funding from the Ministry of Environment and Food of Denmark through the Green Development and Demonstration Program (GUDP), project STEER 34009-20-1649. We would like to thank the skipper and crew of the RV Havfisken for their invaluable help during the research cruise and we also want to express our gratitude to Gregers Baungaard and Thyge Baungaard from MLD, Esbjerg, Denmark for the technical assistance they provided during the trials.

References

Akaike, H., 1974. A new look at the statistical model identification. IEEE Trans. Automat. Control 19 (6), 716–723.
Amoroso, R.O., Pitcher, C.R., Rijinsdorp, A.D., McConnaughey, R.A., Parma, A.M., Suuronen, P., Eigaard, O.R., et al., 2018. Bottom trawl fishing footprints on the world's continental shelves. Proceedings of the National Academy of Sciences U.S.A. 115, E10275–E10282.
Balash, C., Blake, W., Sterling, D., 2020. Seeking maximum effectiveness and efficiency for large multi-sail penaeid otter boards. Ocean Eng. 200 https://doi.org/10.1016/j.oceaneng.2020.107093.
Barton, K., 2022. MuMIn: Multi-Model Inference. R Package Version 1.46.0. https://CRAN.R-project.org/package=MuMIn.
Bates, D., Maechler, M., Bolker, B., Walker, S., 2014. lme4: Linear Mixed-Effects Models Using Eigen and S4. R Package Version 1.1-7. http://CRAN.R-project.org/package=lme4.
Chu, W., Chen, G., Ye, X., Cui, X., 2020. Hydrodynamic performance and structural response characteristics of the double-slotted vertical cambered V-Type otter board. Aquac. Fish. 5, 201–209.
DeLouche, H., Legge, G., 2004. Reducing seabed contact while trawling: a semi-pelagic trawl for the Newfoundland and Labrador shrimp fishery. St. John's, Newfoundland A Report Submitt. Canadian Center Fisheries Innov. 84, 96.
Eayrs, S., 2014. Evaluating the efficacy of semi-pelagic otter boards to reduce environmental impact and improve profitability in the New England ground fish fishery: a win-win for fishermen and the environment. Northeast Consortium, University of New Hampshire Collab. Fisheries Res. Fellowship Rep. 27.
Eayrs, S., Thorbjornson, T., Ford, J., Deese, H., Smith, G., 2012. Saving fuel to increase profitability and reduce environmental impact in a U.S. ground fish fishery. In: Second International Symposium on Fishing Vessel Energy Efficiency. E-Fishing. Vigo, Spain,May 2012, p. 10.
Eayrs, S., Craig, T., Short, K., 2020. Review of Mitigation Techniques to Reduce Benthic Impacts of Trawling. MIT2019-02 Final Report Prepared by Terra Moana Limited for the Conservation Services Programme. Department of Conservation, p. 135.
FAO, 2018. The State of World Fisheries and Aquaculture 2018. Food and Agricultural Organization, Rome.
Grimaldo, E., Pedersen, R., Sistiaga, M., 2015. Energy consumption of three different trawl configurations used in the Barents Sea demersal trawl fishery. Fish. Res. 165, 71–73.
He, P., Hamilton, R., Littlefield, G., Syphers, R., 2006. Design and test of a semi-pelagic shrimp trawl to reduce seabed impact. In: Final Report Submitted to the Northeast Consortium. UNH-FISH-REP-2006-029. University of New Hampshire, Durham, NH.
Lee, J., Yoon, H., Park, Y., Choi, K., Lee, Ch, Shim, D., Park, S., 2019. Design and fabrication of fluid flow characteristic controllable trawl door using a trailing edge flap. J. Mech. Sci. Technol. 33, 5623–5630.
Liu, J., Huang, H.L., Li, L.Z., Qu, T.C., Wu, Y., Chen, S., Yang, J.L., Rao, X., 2017. Hydrodynamic characteristics of the oval cambered double slotted otter board in bottom trawl fisheries. IOP Conf. Ser. Earth Environ. Sci. 77, 012012.
Mellibovsky, F., Prat, J., Notti, E., Sala, A., 2018. Otterboard hydrodynamic performance testing in flume tank and wind tunnel facilities. Ocean Eng. 149, 238–244.
McHugh, M.J., Broadhurst, M.K., Sterling, D.J., Millar, R.B., 2015. Comparing three conventional penaeid-trawl otter boards and the new batwing design. Fish. Res. 167, 180–189.
O'Neill, F.G., Summerbell, K.D., 2016. The hydrodynamic drag and the mobilisation of sediment into the water column of towed fishing gear components. J. Mar. Syst. 164, 76–84.
O'Neill, F.G., Summerbell, K., 2011. The mobilisation of sediment by demersal otter trawls. Mar. Pollut. Bull. 62, 1088–1097.
Patterson, H.D., Thompson, R., 1971. Recovery of inter-block information when block sizes are unequal. Biometrika 58, 545–554.
Pérez Roda, M.A., Gilman, E., Huntington, T., Kennelly, S.J., Suuronen, P., Chaloupka, M., Medley, P., 2019. A Third Assessment of Global Marine Fisheries Discards. FAO, Rome, p. 78. FAO Fisheries and Aquaculture Technical Paper No. 633.
Prat, J., Antonijuan, J., Folch, A., Sala, A., Lucchetti, A., Sardà, F., Manuel, A., 2008. A simplified model of the interaction of the trawl warps, the otterboards and netting drag. Fish. Res. 94, 109–117.
R Core Team, 2020. R: A Language and Environment for Statistical Computing. R Foundation for Statistical Computing, Vienna, Austria. http://www.R-project.org/.
Reite, K.-J., Sørensen, A., 2006. Mathematical modelling of the hydrodynamic forces on a trawl door. J. Ocean Eng. 31, 432–453.
Reite, K.-J., Sørensen, A.J., 2004. Hydrodynamic properties important for control of trawl doors, 2004. In: Katebi, R., Longhi, S. (Eds.), Control Applications in Marine Systems. International Federation of Automatic Control, Ancona, Italy, pp. 143–148.
Sala, A., Farran, J., Antonijuan, J., Lucchetti, A., 2009. Performance and impact on the seabed of an existing- and an experimental-otterboard: comparison between model testing and full-scale sea trials. Fish. Res. 100, 156–166.
SEAFISH, IFREMER, DIFTA, 1993. Otterboard Performance and Behaviour. Commission of the European Communities FAR, p. 159.
Shen, X., Hu, F., Kumazawa, T., Shiode, D., Tokai, T., 2015. Hydrodynamic characteristics of a hyper-lift otter board with wing-end plates. Fish. Sci. 81, 433–442.
Sistiaga, M., Herrmann, B., Grimaldoa, E., Larsen, R.B., Tatone, I., 2015. Effect of lifting the sweeps on bottom trawling catch efficiency: a study based on the Northeast arctic cod (*Gadus morhua*) trawl fishery. Fish. Res. 167, 164–173.
Sterling, D., Eayrs, S., 2010. Trawl-gear innovations to improve the efficiency of Australian prawn trawling. Vigo, Spain. In: First International Symposium on Fishing Vessel Energy Efficiency E-Fishing, p. 5.
Su, X., Lu, H., Feng, B., Chen, Q., Yan, Y., 2018. Hydrodynamic characteristics of the double-winged otter board in the deep waters of the Mauritanian Sea. J. Oceanol. Limnol. 36, 1417–1424.
Takahashi, Y., Fujimori, Y., Hu, F., Shen, X., Kimura, N., 2015. Design of trawl otter boards using computational fluid dynamics. Fish. Res. 161, 400–407.
Wang, G., Huang, L., Wang, L., Zhao, F., Li, Y., Wan, R., 2021. A metamodeling with CFD method for hydrodynamic optimizations of deflectors on a multi-wing trawl door. Ocean Eng. 232 https://doi.org/10.1016/j.oceaneng.2021.109045.
Wang, L., Wang, L., Feng, C., Zhou, A., Yu, W., Zhang, Y., Zhang, X., 2017. Influence of main-panel angle on the hydrodynamic performance of a single-slotted cambered otter-board. Aquacult. Fish. 2, 234–240.
Wang, L., Zhang, X., Wan, R., Xu, Q., Qi, G., 2022. Optimization of the hydrodynamic performance of a double-vane otter board based on orthogonal experiments. J. Mar. Sci. Eng. 10, 1177. https://doi.org/10.3390/jmse10091177.
Xu, Q.C., Feng, C.L., Huang, L.Y., Xu, J.Q., Wang, L., Zhang, X., 2018. A comparative study on hydrodynamic performance of double deflector rectangular cambered otter board. J. Ocean Univ. China 17, 1218–1224.
Xu, Q., Huang, L., Li, X., Li, Y., Zhao, X., 2021. Parameter optimization of a rectangular cambered otter board using response surface method. Ocean Eng. 220 https://doi.org/10.1016/j.oceaneng.2020.108475.
You, X., Hu, F., Zhuang, X., Dong, S., Shiode, D., 2021. Effect of wingtip flow on hydrodynamic characteristics of cambered otter board. Ocean Eng. 222, 108611.
Zhang, X., Wang, M., Wang, J., 2004. Hydrodynamic characteristics of vertical V type otter board. J. Fish. China 3, 311–315.
Zhuang, X., You, X., Kumazawa, T., Shiode, D., Takahashi, Y., Hu, F., 2022. Effect of spanwise slit on hydrodynamic characteristics of biplane hyper-lift trawl door. Ocean Eng. 249 https://doi.org/10.1016/j.oceaneng.2022.110961.
Zuur, A.F., Ieno, E.N., 2016. A protocol for conducting and presenting results of regression-type analyses. Methods Ecol. Evol. 7, 636–645. https://doi.org/10.1111/2041-210X.12577.
Zuur, A.F., Hilbe, J.M., Ieno, E.N., 2013. Beginner's Guide to GLM and GLMM with R. Highland Statistics Ltd, Newburgh.
Zuur, A.F., Ieno, E.N., Elphick, C.S., 2010. A protocol for data exploration to avoid common statistical problems. Methods Ecol. Evol. 1, 3–14.